Study of Transient Simulation for Solar Heating System

Dr. Sabah Tarik Ahmed*, Dr. Qussai Jihad Abdul-Ghafour* & Laith Abdulmonem. Ismael*

Received on: 1/11/2009
Accepted on: 3/2/2011

Abstract

In the current study simulation method was used for design of solar water heating system. An integrated transient simulation program was built up for simulating the Iraqi solar house heating system using TRNSYS as a design tool.
The modeling was carried out is modeled for other virtual solar heating systems similar to the Iraqi solar house. The results obtained were used to develop a general design procedure for solar heating systems in Baghdad.
Using the design charts and TRNSYS as a design tool simplifies the designer's task for predicting the long - term heating energy supplied from a solar collector array.
The above simulation was applied for Iraqi solar house and the results gave the increasing in storage volume caused increase the auxiliary energy supplied to the system. So, the best practical storage volume is $20m^3$ and increasing the collector area to optimum value results in increasing the solar fraction (f). The solar fraction may reach 0.97 when the collector area becomes as $400m^2$ at storage volume of $20m^3$.

Keywords: Solar Heating, Solar fraction, Storage, TRNSYS.

دراسة في نمذجة الحالة الانتقالية لمنظومة تدفئة تعمل بالطاقة الشمسية

الخلاصة

تم بناء برنامج حاسوبي متكامل لنمذجة الحالة الانتقالية لأداء منظومة التدفئة الشمسية للبيت الشمسي العراقي باستخدام ترانزس (TRNSYS) كأداة للتصميم . وتم توظيف البرنامج لنمذجة عدد من المنظومات الافتراضية المشابهة لمنظومة البيت الشمسي العراقي . واستخدمت نتائج النمذجة لاستحداث طريقة عامة لتصميم منظومة التدفئة الشمسية لمدينة بغداد .
إن استخدام المخططات التصميمية الحالية والنمذجة باستخدام ترانزس (TRNSYS) يسهل مهمة المصمم للتنبؤ بقيمة حمل التدفئة المجهزة من المنظومة الشمسية خلال فترة اشتغال طويلة (شهرية أو موسمية).
إن النتائج المستحصلة من عملية النمذجة التي أجريت على البيت الشمسي العراقي توجز إن الزيادة في حجم الخزان تسبب انخفاض تتبعه زيادة في قيمة الطاقة المضافة للمنظومة (Auxiliary energy) وعليه فقد وجد إن الحجم العملي الأفضل للمنظومة هو $20\ m^3$ و إن الزيادة في مساحة المجمع الشمسي تؤدي إلى زيادة في قيمة الكسر الشمسي(f) والذي قد تصل قيمته إلى (0.97) عندما تكون مساحة المجمع الشمسي $400m^2$ وحجم الخزان $20m^3$.

* Machines & Equipments Engineering Department, University of Technology/ Baghdad

Introduction

Liquid-based solar heating systems Fig.1 are currently more common than the air heating systems. This is because liquid system components are easy to transport and they are superior on a volume basis to any other practical, sensible heat storage material. The disadvantages of the liquid system however, are that heat exchange with the building air is required and precautions against freezing, boiling, and corrosion must be taken. This is essential because a fluid leak in liquid systems could cause extensive damage, while this problem does not encounter in air system.

The solar collectors are used to transform incident solar radiation into thermal energy. This energy is stored in a form of sensible heat in a liquid storage tank. The storage energy provides all or some of the heat required to meet required heating load. Because the heat available from the solar collectors does not always match the demand, the heat stored will be depleted frequently, and the need for auxiliary heating becomes essential to meet the heating load required for building.

A brief review and discussion of some of the published works on solar heating system and components are described in the following sections.

1. Mathematical modeling

In order to simulate the transient state of a solar system, it is necessary to study such a system in an arbitrary short time step. Hourly performance has been found convenient and reasonable for simulation. The mathematical expressions for each component must then be prepared for such a time step in detail.

3.1Calculation of Solar Radiation on a Tilted Surface

Hourly radiation data on a horizontal surface is available for many locations in the world. However, radiation data on tilted surfaces is generally not available.

The first step in calculation solar radiation on a tilted surface is to break down the horizontal data into beam and diffuse components. This is accomplished using the correlation by Erbs [1] which relates I_d / I with the clearness index k_T. The correlation is:

$$\left[\frac{I_d}{I}=\begin{cases}1-0.09*k_T & k_T\le 0.22\\ 0.9511-0.16*k_T+4.388*(k_T)^2-16.638*(k_T)^3 & \\ +2.336*(k_T)^4 & 0.22<k_T\le 0.8\\ 0.165 & k_T>0.8\end{cases}\right] \quad ....(1)$$

$$k_T=\frac{I}{I_o} \quad ....(2)$$

The diffuse component I_d can be estimated from Erbs [1] correlation, then the beam component I_b can be calculated by:

$$I_b = I - I_d \quad \ldots(3)$$

The next step is to calculate hourly radiation on a tilted surface I_T as follows [2]:

$$I_T = R * I \quad \ldots(4)$$

Where R, is the ratio of the hourly radiation on a tilted surface to that on a horizontal surface. The incident radiation has three different spatial distributions: beam radiation, diffuse sky radiation, and diffuse ground – reflected radiation. Assuming diffuse radiation to be isotropic "i.e. uniformly distributed over sky dome", R can be expressed by [2]:

$$R=\left(1-\frac{I_d}{I}\right)*R_b+\frac{I_d}{I}*\frac{(1+\cos\beta)}{2}+\rho_g*\frac{(1-\cos\beta)}{2} \quad ....(5)$$

3.2Performance of Solar Collectors

A general expression for collector efficiency can be obtained from the Hottel- Wilier- Bliss equation [3] as:

$$\eta = \frac{Q_u}{Ac\, I_T} = F_R(\tau\alpha)_n - F_R U_L \frac{T_i - T_a}{I_T} \quad ...(6)$$

Collector test results are often presented as straight line plots of η versus $(T_i - T_a) / I_T$ with intercept of $F_R (\tau\alpha)_n$ and slope $- F_R U_L$.

Collector tests are generally performed on clear days at normal incidence, so that the transmittance – absorptance product is nearly the normal incidence value for beam radiation, $(\tau\alpha)_n$. The intercept efficiency $F_R (\tau\alpha)_n$, is corrected for non-normal solar incidence by the factor $(\tau\alpha) / (\tau\alpha)_n$. By definition, $(\tau\alpha)$ is the ratio of the total absorbed radiation to the incident radiation. Thus, a general expression for $(\tau\alpha) / (\tau\alpha)_n$ is [4]

$$\frac{(\tau\alpha)}{(\tau\alpha)_n} = \frac{Ib_T \frac{(\tau\alpha)_b}{(\tau\alpha)_n} + I_d \left(\frac{1+Cos\,\beta}{2}\right)\frac{(\tau\alpha)_{sky}}{(\tau\alpha)_n} + \rho_g * I_T \left(\frac{1-Cos\,\beta}{2}\right)\frac{(\tau\alpha)_g}{(\tau\alpha)_n}}{I_T}$$

....(7)

All of the analysis is common for all types of collectors except for the calculation of $(\tau\alpha)/(\tau\alpha)_n$. The correction for this term for flat plate collectors is obtained by using the incidence angle modifier [5].

3.3 Storage Tank Performance

The thermal performance of fluid-filled sensible energy storage tank, subject to thermal stratification can be modeled by assuming that the tank consist of N fully-mixed equal volume segments, as shown in Fig. 2 . The degree of stratification is determined by the value of N. If N is equal to 1, the storage tank is modeled as a fully-mixed tank and no stratification effect are possible.

In general, the storage tank has two fluid loops, a collector loop and a load loop. The load flow enters at the bottom of the tank and the hot source stream enters at the top of the tank. At the end of each time interval, any temperature inversions that exist are eliminated by total mixing of the appropriate adjacent nodes. The overall loss from any node occurs from the tank to the surrounding [6]. The overall conductance for heat loss based on environmental temperature T_{env} must be specified, and then divided among the nodes.

An assumption is to assume that the fluid streams flowing up and down from each node are fully mixed before they enter each segment. With reference to Fig. 3, this implies that $\dot{m}_1$ is added to $\dot{m}_4$ and $\dot{m}_2$ is added to $\dot{m}_3$, and a resultant flow, either up or down, is determined. An energy balance on the i^{th} segment (neglecting losses) is then [7], [8]:

$$M_i \, cp_f \frac{dT_i}{dt} = \begin{cases} (\dot{m}_1 - \dot{m}_3) cp_f (T_{i-1} - T_i) & \dot{m}_1 \geq \dot{m}_3 \\ (\dot{m}_3 - \dot{m}_1) cp_f (T_{i+1} - T_i) & \dot{m}_1 < \dot{m}_3 \end{cases} \quad ...(8)$$

An energy balance written for the i^{th} tank segment including energy loss is:

$$M_i cp_f \frac{dT}{dt} = \alpha_i \dot{m}_h cp_f (T_h - T_i) + \beta_i \dot{m}_L cp_f (T_L - T_i) + UA_i (T_{env} - T_i) + \gamma_i * (T_{i-1} - T_i) * cp_f \quad if\ \gamma_i > 0 \quad ...(9)$$

$$+ \gamma_{i+1} * (T_i - T_{i+1}) * cp_f \quad if\ \gamma_{i+1} < 0$$

Where

$$\alpha_i = \begin{cases} 1 & if \quad i = S_h \\ 0 & otherwise \end{cases} \quad .... \ (10)$$

$$\beta_i = \begin{cases} 1 & if \quad i = S_L \\ 0 & otherwise \end{cases} \quad ....(11)$$

$$\gamma_i = \dot{m}_h \sum_{j=1}^{i-1} \alpha_j - \dot{m}_L \sum_{j=1+1}^{N} \beta_j \quad ....(12)$$

The temperature of each of the N tank segments is determined by the integration of their time derivatives expressed in above equations.

Energy flows and the change in internal energy are calculated as follows:

$$\dot{Q}_{env} = \sum_{i=1}^{N} UA_i (T_i - T_{env}) \quad ....(13)$$

$$\dot{Q}_s = \dot{m}_L cp_f (T_1 - T_L) \quad ....(14)$$

$$\dot{Q}_{in} = \dot{m}_h cp_f (T_h - T_N) \quad ...(15)$$

$$\Delta E = V * \rho_f$$

$$* cp_f [\sum_{i=1}^{N} T_i - \sum_{i=1}^{N} T_i|_{t=time(0)}] / N \quad ....(16)$$

3.4 Pressure Relief Valve

Solar energy systems which use a liquid such as water for a heat transfer medium typically include a pressure relief valve to discard the steam if the liquid begins to boil as shown in Fig. 1.

The model monitors inlet temperature, flow rate, and a comparison temperature T_{romp} . Energy discarded at a rate $\dot{Q}_{boil}$ whenever T_{comp} greater than T_{boil} which is the boiling point of the liquid. Loss of mass when the valve is open is assumed negligible and the outlet flow rate is always equal to the inlet flow rate [7], [8], [9].

So if $T_i > T_{boil}$ then

3.5 Pump Performance and Control

The pump controller showed in Fig. 1.generates a control function γ_o which can have values of 0 or 1. The value of γ_o is chosen as a function of the difference between upper and lower temperatures (collector outlet temperature T_h, and the lower layer temperature of the storage tank T_L). These are compared with two dead band temperature differences, ΔT_h and ΔT_L . The new value of γ_o depends on whether the input control function γ_i equal to 0 or 1. The controller is normally used with γ_o connected to γ_i giving a hysteresis effects [10]. The pump controller function is shown graphically in Fig.4. Mathematically, this expressed as:

$$\dot{Q}_{boil} = \dot{m}_c \ cp \ (T_i - T_{boil}) \quad ....(17)$$

$$T_o = T_{boil} \quad ....(18)$$

otherwise

$$\dot{Q}_{boil} = 0 \quad .. .(19)$$

$$T_o = T_i \quad ....(20)$$

$$If \ \ \gamma_i = 1 \ and \ \Delta T_L \le (T_h - T_L), \ \gamma_o = 1 \quad ....(21)$$

$$If \ \ \gamma_i = 1 \ and \ \Delta T_L > (T_h - T_L), \ \gamma_o = 0 \quad ....(22)$$

$$If \ \ \gamma_i = 0 \ and \ \Delta T_h \le (T_h - T_L), \ \gamma_o = 1 \quad .....(23)$$

$$If \ \ \gamma_i = 0 \ and \ \Delta T_h > (T_h - T_L), \ \gamma_o = 0 \quad .....(24)$$

In many solar energy systems, there is no continuous flow modulation and the control function is either 0 or 1. In this case, the outlet flow rate and the power used are either both zero or both at their maximum values [10].

It is assumed that addition of heat to the fluid by the pump is neglected i.e

$$T_o = T_i \quad ...(25)$$

$$\dot{m}_o = \gamma_o \dot{m}_{max} \quad ....(26)$$

4. The Building under Study

The solar guest house has a total area of 600 m^2 with a solar air-conditioned area of 400 m^2. It includes a reception room, a dining room, four bedrooms, two bathrooms, a kitchen and a machinery room. Fig.5 shows the house layout diagram, [11].

The total heat loss coefficient of the building walls are calculated as 0.66 W / m^2. $^\circ$C.. The heat loss coefficient for the roof was calculated as 0.573 W / m^2.$^\circ$C.

4.1 Building Heating Load

The air-conditioning heating load calculated by the traditional method; based on temperature difference between outside and inside temperature [15]. The house heating load was determined and found to be 14.124 kW based on 22 $^\circ$C inside temperature and 2 $^\circ$C ambient temperatures.

4.2 Heating System Equipment and Operation

The system consists of two loops. Solar collectors loop & heating Loop.

The solar collectors loop consists of:-

a. 128 flat-plat collectors are with single glass covers of 1.89 m^2 area each, and a total effective area is of 243 m^2. They are oriented at 22.5 $^\circ$ east of south with a summer operation tilt angle of 17°. The performance parameters of the collector used are, $F_R (\tau\alpha)_n$ = 0.771, $F_R U_L$ = 15.25 kJ/hr. m^2.$^\circ$C (4.236 kW / m^2.$^\circ$C). An incidence angle modifier b_o = -0.1.

b. A 20 m^3 (84 kg / m^2 of collector) stainless steel hot water storage tank. It is of a rectangular type with dimensions of (2*4.3*2.3 m). Fiber glass insulation material of 10 cm thickness was used to minimize its heat loss.

c. Two heat collection circulating pumps "one standby" with a flow rate capacity of 3.78 ℓ / sec each.

d. Pressure relief valve mounted on the main delivery pipe from the collector array.

e. On-off controller for circulating pump actuated when the temperature difference across the collector array exceeded 3 $^\circ$C and stopped when this difference is less than 0.5 $^\circ$C.

The Heating Loop Consist of the following:

a. Fan coil unit distributed as the follows:

2 units in the living room with a capacity of 2.556 kW

2 units in the dining room with a capacity of 2.556 kW

4 units in the bed room with a capacity of 2.556 kW

2 units in the entrance with a capacity of 1.929 kW

b. Auxiliary kerosene boiler with a capacity of 29 kW.hr used to supply the system with the required hot water when the solar storage energy is not sufficient.

c. Fresh air system which consists of one air handling unit with a capacity of11.12 KW and an exhaust fan used to heat and distribute the fresh air in the house.

d. Two hot water circulating pumps with 1.82 L/sec flow rate capacity each (one standby) used to circulate the hot water between the storage tank or the auxiliary boiler and the fan coil unit.

e. A motorized 3-way valve, used to control the hot water Flow between the storage tank and the auxiliary boiler

4.3 Assumptions for simulation

The assumptions which are necessary to build up an integrated system for computer simulation are based on empirical and experimental results taken from the solar heating field researchers. The assumptions are:-

1. The solar fraction is taken to be the part of kerosene boiler that can be covered by the solar system. Power consumption by other equipment (circulating pump, fan motors, controllers) are excluded [13].
2. The mass flow rate per unit collector area is 50 kg / hr.m2 [5].
3. Storage tank height to diameter ratio is equal to 0.33, with three layers for stratification, and insulated with 10 cm thickness of fiber glass [14], [15]. With over all heat transfer coefficient equal to (0.316 W/m.^{o}c)
4. Pressure relief valve is actuated when the collector outlet temperature exceeded 96 $^{\circ}$C for preventing steam formation, [8], [15], and [14].
5. The circulation pump in the collector water loop operates when the temperature difference between the collector outlet water and the top layer temperature of the storage tank exceeds 3 $^{\circ}$C and stops when the difference becomes lower than 0.5 $^{\circ}$C [11], [14], [15], [4], [10].
6. Water supply and return pipe length, diameters and insulation thickness are directly proportional with the collector array area.

4.4 The Solar Heating System Presentation by TRNSYS

Knowing the performance of each component and the TRNSYS approach of calling each system component [8][16], it is safe now to build up an assembly for the whole system. Figure 6 shows a schematic block diagram for the solar heating system presented by TRNSYS. This diagram is the first step which simplifies making the simulation deck. The solar house characteristics, weather data and the location are used in the main program , and the block diagram, Fig.6.

4.5 The Main Program

The main program is organized to simulate virtual systems which may be larger or smaller than the Iraqi solar house but similar in application.

The steps in arranging the main program are the following;

1. Selecting a number of different building sizes i.e. different cooling loads, by scaling the solar house heating load.
2. Choosing different collector areas, starting from 40 m^2 to 240 m^2 with 40 m^2 increments. The idea behind this step is studying the effect of collector array area on the solar fraction and hence the overall system performance.
3. Choosing different storage sizes in order to get the minimum allowable size, based on minimizing the energy discarded from the pressure relief valve. The storage volume was changed from 25 to 200 liter per square meter of collector area with 25 l /m^2 increments.
4. Changing the collector area means that the piping length, diameter and insulation

thickness are also changed. So the overall energy loss coefficient from piping U_{Ploss} is also changed. The program calculating U_{Ploss} before using it when calling TRNSYS.

5. TRNSYS need starting initial values to start the simulation. These values are not easily predicted and errors in limiting these values are expected. For rounding this error the simulation strategy is started two days before the recommended day, and the results are taken from the third day onwards. Fig 7. Shows a flow diagram for the solar heating system.

5. Result and Discussion

5.1 The Overall Solar System Thermal Performance

The first result obtained from the simulation of solar heating system is the overall energies behind it. Fig 8shows the hourly incident radiation, useful energy, auxiliary energy and heating load for the recommended day of January at 17^o tilt angle and -22.5^o azimuth angle , similarly for the other winter months.

One could notice from data for January Fig 8 and December Fig 9, the total collected energy was not completely consumed before using the auxiliary energy. No auxiliary energy is consumed in February and November which means that the solar fraction obtained from solar system is 100%.

5.2Effect of collector area

Numbers of simulations are made for different collector areas, assuming a collector tilt angle of 17^o from horizontal, a storage size to area ratio is 83 l/m^2 and a water flow rate through the collector equal to 56 kg/h per m^2 of collector. These data are identical to building data[11]. The results of the simulations were used to plot graphs relating the annual solar fraction (f)(the fraction of heating load covered by the solar system) and the design collector to building area factor CAF. The results scheduled in table (1) and graphically in Fig10.The curve has an equation:

$$f=1.215(A_c/A_b)^4 - 2.34(A_c/A_b)^3+0.3585(A_c/A_b)^2 +1.73(A_c/A_b)-2*10^{-5} \ldots.(27)$$

The collector area factor (CAF) for the Iraqi solar house is equal to (0.61), using this number in Fig 10. Or in eq27 , the obtained solar fraction is (0.82) . This result close to the actual one obtained by [11] .This approach is considered useful because it offers the flexibility to the designer to base his design on either of the parameters and do some kind of cross-checking in determining the optimum collector area of a solar space heating system.

5.3Effect of Changing of Collector Parameters

Several methods for characterizations, or collector models, have various number of parameters and are thus of varying complexity, and they serve different purposes. At one extreme very detailed model include all of the design features of the collector (plate thickness, tube spacing number of covers, cover material and back and edge insulation dimensions, etc). At another extreme is a model that includes only two parameters, one shows how the collector absorbs radiation and the other how it loses heat. $F_R(\tau\alpha)_n$ is an indication of how energy is absorbed and $F_R U_L$ is an indication of how energy is lost. These two parameters constitute the simplest collector model.

The simulation in previous section was repeated for another two types of collectors [7]; table 2 shows the three types of collector used in this simulation to explain its effect on system performance. The results obtained for the three types of collectors are scheduled in table (3) and graphically shown in Fig.11, and Fig.12. It is clear that the collector of type (A) gives higher solar fraction Fig.11 .and lower auxiliary energy consumed Fig 12.

5.4Best Size Selection for Solar Space Heating System

The auxiliary energy is a function of the solar energy collected by the solar system, therefore ,the monthly auxiliary energy requirement was determined as a function of the storage size as well as solar collector area , as shown in Fig13.For a given storage volume . The auxiliary energy requirement decrease rapidly with increasing solar collector area until a collector area is reached where the slope of the curve flattens out. Fig13 displays that selective storage size of 20 m^3 gives minimum auxiliary energy required. These result matches the solar system data shown in ref [11]

It is also of interest to know the solar fraction that can be provided by solar energy. Fig 14 shows the daily percent of solar fraction (f) as a function of the solar collector area for different storage size. For affixed solar collector area, the increasing of storage volume from 20m^3 to70 m^3 signification decrease the percent of the fractional energy that is provided by solar energy. Increasing the collector area to optimum value, results in increasing the solar fraction. The solar fraction may reach 0.97 when the collector area becomes as 400m^2 at storage volume of 20m^3. The vertical dashed line shown in Fig.13 and Fig.14 is for the actual collector area used. It is clear that the optimum value of the auxiliary energy closed to the corresponding value obtained from the simulation [11].

5.5Influence of storage size on solar system performance

The thermal energy storage (TES) can be defined as the temporary storage of thermal energy at high or low temperatures. Energy storage can reduce the time or rate mismatch between energy supply and energy demand, and it plays an important role in energy conservation so the volume of storage is an important parameter for the solar system. This section uses the amount of storage volume to study its effect on the whole system performance. The data used are, collector area is (243m^2) and the slope of collector angle is set at (17^o) and (-22.5^o) azimuth angle.

The resultant data are scheduled in table 4 and graphically observed in Fig.15 and Fig.16.The resultant curve for Fig 15 has an equation of:

$$f = -4*10^{-7}V_t^4+6*10^{-5}V_t^3-0.0032V_t^2+0.0669V_t+0.33 \quad \ldots(28)$$

And Fig.16 curve has an equation of:

$$Q_{aux}= 0.0002V_t^6-0.0502V_t^5+4.386V_t^4-197.86V_t^3+4869.3V_t^2-61335Vt+351209 \quad \ldots(29)$$

Equating the first derivate of equation 28 or 29 to zero yields an optimum storage size.

These results show that the (20m^3) is close to the standard and the practical tank size.

The increase of storage volume(as shown in figs 15and 16) reverse proportional with solar fraction (f) due to decrease temperature supply to load, and increase the amount of heat lost due to enlarging the storage tank surface area.

6. References

[1]Erbs, D.G., "Method for estimating the diffuse fraction of hourly, daily and monthly average global solar radiation", M. Sc. thesis in Mechanical Engineering, University of Wisconsin – Madison, (1980).

[2]Kuchler, T.M., "Evaluating model to predict insolation on tilted surfaces", Solar Energy, Vol. 23, p. 111, (1979).

[3]Hottel, H.C. and Whillier, A., "Evaluation of flat– pate solar collector performance". Trans. of the conference on the use of solar energy, II, Thermal Processes, 74 –104, University of Arizona,(1955).

[4]Klein S.A, "Calculation of the monthly – average transmittance – absorptance product", Solar Energy, Vol. 23, p. 547, (1979).

[5]ASHRAE standard 93 – 77, "Method of testing to determine the thermal performance of Solar collectors", New York (1977).

[6]Lavan, Z. and Thompson, T., "Experimental study of thermally stratified hot water storage tanks", Solar Energy, Vol. 19, p. 519, (1977).

[7]Duffie, J.A. and Beckman, W.A.,. "Solar Engineering of Thermal Processes", John Wiley & Sons, New York, (1980).

[8]Klein, S.A. et al. 2008. TRNSYS, a Transient Simulation Program. Solar Energy Laboratory, University of Wisconsin.

[9]Lunde, Peter J., "Solar Thermal Engineering", John Wiley and Sons, New York (1980).

[10]Piessens, L.P, "A microprocessor control component for TRNSYS", M. Sc. Thesis, University of Wisconsin – Madison, (1980).

[11]AL– Karaghouli, A., AL – Hamdani, N. and AL – Sinan, W., " Iraqi Solar house heating season performance evaluation", Solar and Wind Technology, Vol. 6, No.1, pp.29 – 40, (1989).

[12]ASHRAE Handbook for Fundamental 2008.

[13]Klein, S.A. and, Beckman, W.A. and Duffie, J.A. "Solar Heating Design By The f – Chart Method, John Wiley & Sons, Inc., (1977).

[14]Ward, Dan S., Oberoi, Harjinder S. and Weinstein, Stephen D., "How to solve material and design problems in Solar heating and cooling", Noyes data Corporation, (1982).

[15]Solar Heating and Cooling in Japan "Product and System Date Manual (1980)", Tech- in Nots,YAZAKI company .

[16]Q.J. Abdul-Ghafour "Development of design charts for solar cooling system" PhD thesis, university of Baghdad/ mechanical engineering department (2001).

Nomenclature

Symbol	Meaning	Unit
A	Collector aperture area	m^2
c_p	Specific heat of collector fluid	kJ/ kg. K
F_R	Heat removal factor	-
H	Daily solar radiation	W/ m^2
HL	Heating load	W.
I	Hourly total radiation on a horizontal surface	MJ/ m^2
I_o		
k_T	Clearness index	-
M	Fluid mass	kg
M_D	Month days	
m_h	Fluid mass flow rate to tank from hot source	kg/ s
m_L	Fluid mass flow rate to the load	kg/ s
m_{max}	Maximum pump flow rate	kg/ s
N	Number of fully mixed tank segment	-
n	Number of day in the year	-
Q	Energy	W
R_{th}	Thermal resistance	hr.°C / kJ
T	Temperature	°C
t	Time	sec
U_L	Collector loss coefficient	W/ m^2.°C
U	Over all heat transfer coefficient	W/ m^2.°C
V	Tank volume	m^3

Greek symbols

Symbol	Meaning	Unit
β	Surface tilt angle	degree
γ	Collector azimuth angle	degree
η	Overall collector efficiency	-
ΔE	Change in internal energy	kJ
Δt	time interval	hr
ρ_g	Ground reflectivity = 0.2 for hot season	-
$(\tau\alpha)$	Transmittance – absorptance product	-

Subscripts

Symbol	Meaning
a	ambient
aux	auxiliary
b	beam
bT	beam radiation on tilted surface
boil	Boiling
c	Collector fluid
d	diffuse
env	environment
envcs	Energy loss from piping connecting the solar collectors with the storage tank (hot side)
envsc	Energy loss from piping connecting the storage tank with the collector array (cold side)
f	fluid
g	generator, ground
hw	heating water
L	From load
n	normal
o	outlet from collector
s, sky	sky diffuse
source	supplied to generator
T	on tilted surface
u	useful

Superscripts

Symbol	Meaning
.	Rate of
-	Average

Abbreviations

Symbol	Meaning	Unit
CAF	Collector to building area factor	-
ND	Number of days in the month	-
TES	Thermal energy storage	-

Table 1: Solar Fraction Value versus Collector to Building area (CAF)

A_c / A_{build}	f
0.12	0.21
0.25	0.42
0.38	0.61
0.5	0.74
0.63	0.838
0.75	0.897
0.88	0.94
1	0.967

Table 2: Value of $F_R(\tau\alpha)_n$ and $F_R U_L$ for collectors A, B & C

Collector Type	$F_R(\tau\alpha)_n$	$F_R U_L$ (kJ/m^2.hr. C)
A	0.771	15.25
B	0.73	13.02
C	0.62	11.7

Table 3: Effect of increasing collector area on solar fraction for three types of collector

Ac (m^2)	Ac /A_{build}	Collector A	Collector B	Collector C
50	0.12	0.164708	0.164708	0.118493
100	0.25	0.392058	0.392058	0.316496
150	0.38	0.590603	0.590603	0.489168
200	0.5	0.736248	0.736248	0.633178
250	0.63	0.83967	0.83967	0.740287
300	0.75	0.909439	0.909439	0.817662
350	0.88	0.945805	0.945805	0.879489
400	1	0.973323	0.973323	0.910065

Table 4: Solar Fraction Value at Various Storage Volumes at Collector Area (243m^2)

Storage volume (m^3)	Solar fraction (f)
10	0.737
20	0.82
30	0.789
40	0.752
50	0.713

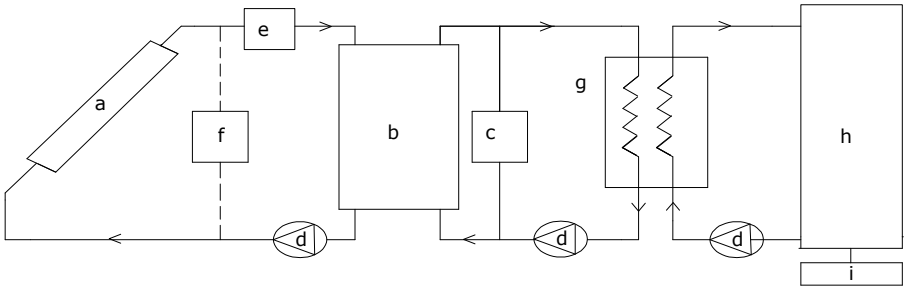

:solar collector, b:storage tank, c:auxiliary heater(series), d:circulation pumps, e:pressure, valve
f: on/off controller, g:heat exchanger, h:building load, e:auxiliary heater (parallel)

Figure 1: Schematic diagram of solar heating system

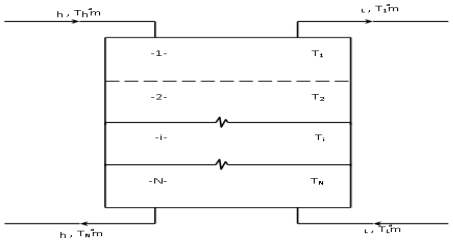

Figure 2: Temperature distribution, energy input and energy output in a fully-mixed, N-equal volume segments storage tank.

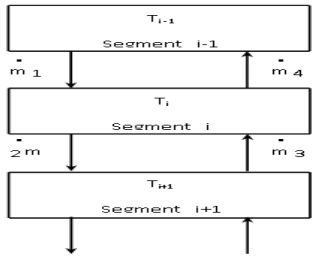

Figure 3: Energy and mass transfer into and from storage tank segment

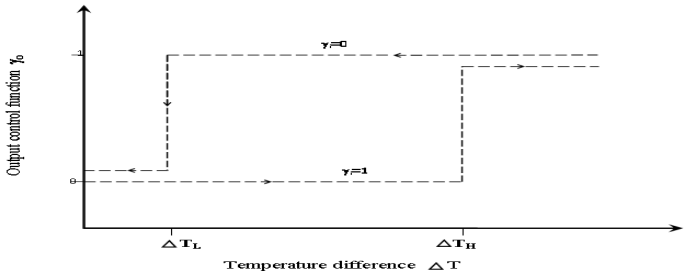

Figure 4: Illustration of the hysteresis effect of the pump controlle

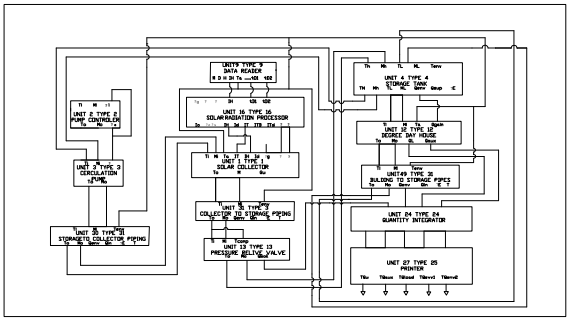

Figure 5: Iraqi solar house layout

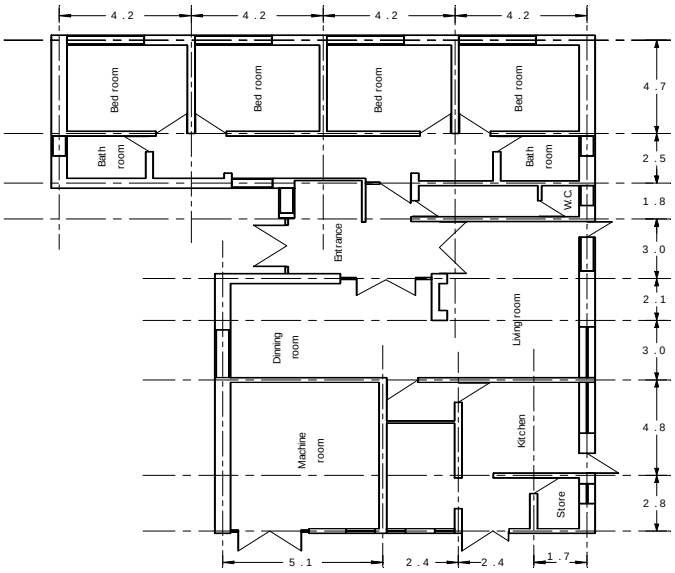

Figure 6: TRNSYS block diagram for Iraqi solar house heating

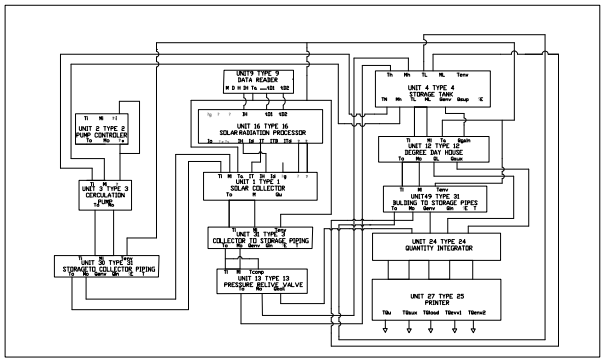

Figure 7: Flow diagram for Iraqi solar house heating system

Transient Simulation of Iraqi Solar Heating System

```
Width 72
        CONSTANTS Clarea = 240  CLMDOT = 13500  STRVOL = 20
CONSTANTS Cap = 126500  TDB = 26.75  TWB = 15.03  CLOAD = 39500.
CONSTANTS TMIN = 80            UPLOSS = UPLOSS
CONSTANTS TAUX = 90    FRTAN = .771          FRUL = 15.25
CONSTANTS TSTEP = DELTIME   LPIPE=LPIPE   DPIPE=DPIPE
CONSTANTS TFIRST = 0   TLAST = 72   CHMDOT= CHMDOT
CONSTANTS DAY-YR = DAY(M)  LAT = 33.3  CLSLOP = 14.6 SHIFT= 0
SIMULATION TFIRST TLAST TSTEP
TOLERANCE - .02       - .02
NOLIST
LIMITS 50  30  50
UNIT 9 TYPE 9 DATA READER
PARAMETERS 8
6   1.0   -5.0   3.6   0.0   6    1    0
UNIT 16 TYPE 16 RADIATION PROCESSOR
        PARAMETERS 6
31 DAY-YR LAT  4871.0   SHIFT
INPUTS 6
9,5   9,19   9,20   0,0   0,0   0,0
0.0   0.0    0.0    0.2   CLSLOP     22.5
UNIT 1 TYPE 1 FLAT PLATE COLLECTOR
PARAMETERS 12
1  1   CLAREA   4.19   1   50    FRTAN   FRUL   0    4.19   1   -0.1
INPUTS 10
30,1   30,2   30,2   9,6   16,6   16,4   16,5   0,0   16,9   16,10
TDB      0      0   TDB   0      0     0      0.2    0   CLSLOP
UNIT 31 TYPE 31 PIPING COLLECTOR TO STORAGE
PARAMETERS 6
DPIPE LPIPE UPLOSS  1000  4.19  TDB
INPUTS 3
1,1    1,2    9,6
TDB    0.0    TDB
UNIT 13 TYPE 13 RELIEF VALVE
PARAMETERS 2
96    4.19
INPUTS 3
31,1    31,2     4,1
30   CLMDOT   20
UNIT 4 TYPE 4 STORAGE TANK
PARAMETERS 8
1 STRVOL  4.19  1000  1.316    0.77    0.77   0.77
INPUTS 5
13,1    13,2    49,1    49,2         9,6
31.5    0.0     80   CHMDOT     TDB
DERVATIVES  3
```

```
TMIN  TMINTMIN
UNIT 2 TYPE 2 PUMP CONTROLLER
PARAMETERS 3
3   3   .25
INPUTS 3
1,1       4,1     2,1
TDB    TMIN    0
UNIT 3 TYPE 3 PUMP
PARAMETERS 1
CLMDOT
INPUTS 3
4,1      4,2    2,1
TMIN    0.0   0.0
UNIT 30 TYPE 31 PIPING STORAGE TO COLLECTOR
PARAMETERS 6
DPIPE  LPIPE  UPLOSS    1000  4.19   TMIN
INPUTS 3
 3,1      3,2    9,6
TMIN    0.0    TDB
UNIT 12 TYPE 12 DEGREE DAY HOUSE
PARAMETERS 6
1, UA, TROOM, H.EMDOT, 4.19, 1150
INPUTS 4
4,3   4,4  9,6    4,5
20,  0.0 , TDB , 0.0
UNIT 49 TYPE 31 PIPING BULDING TO STORAGE
PARAMETERS 6
DPIPE  LPIPE  UPLOSS    1000  4.19   TMIN
INPUTS 3
12,1   12,2   9,6
 20     0.0     TDB
UNIT 24 TYPE 24 QUANTITY INTEGRATOR
INPUTS 7
12,4  1,3  4,5  30,3  31,3 13,3  16,6
0.0     0.0  0.0  0.0   0.0   0.0  0.0
UNIT 27 TYPE 25 PRINTER
PARAMETERS 1
1.0
INPUTS 3
 1,3  12,6  12,3
Qu  Qaux  QLoad
END
```

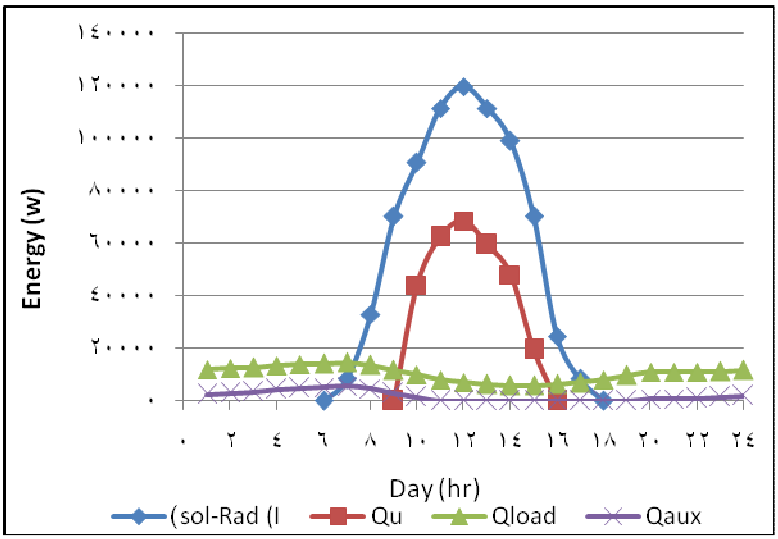

Figure 8: Hourly Variations of incident Solar Energy, useful energy, auxiliary energy& Building Heating Load for January

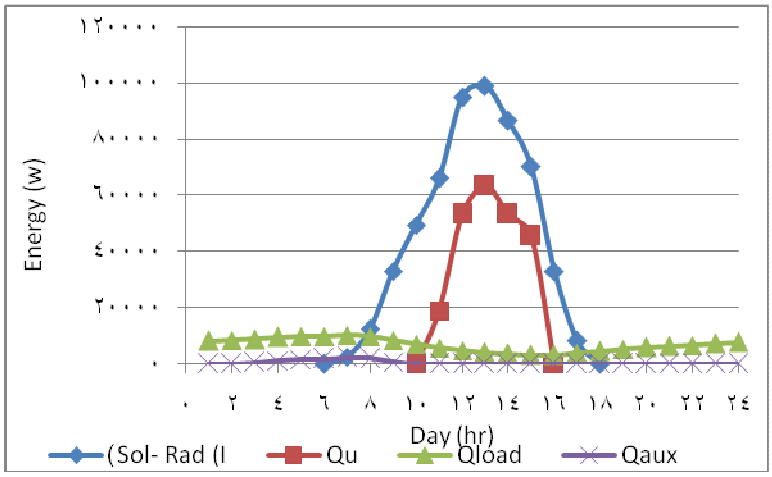

Figure 9: Hourly Variation of incident Solar Energy, useful energy, auxiliary energy &Building Heating Load for

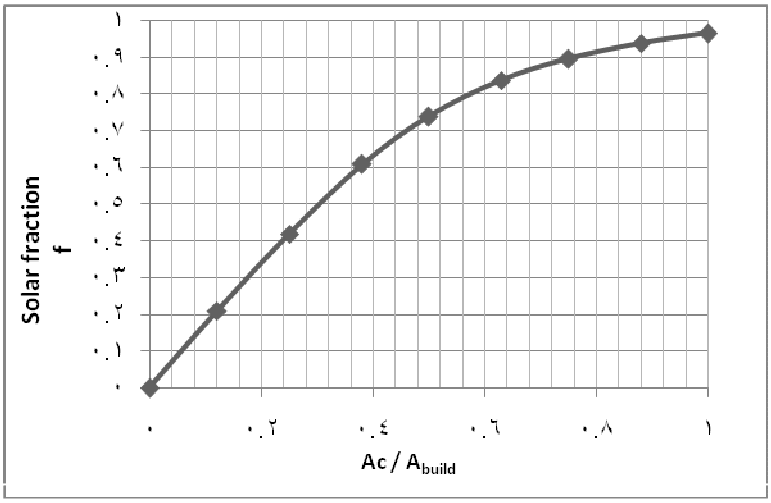

Figure 10: The effect of collector to building area (CAF)

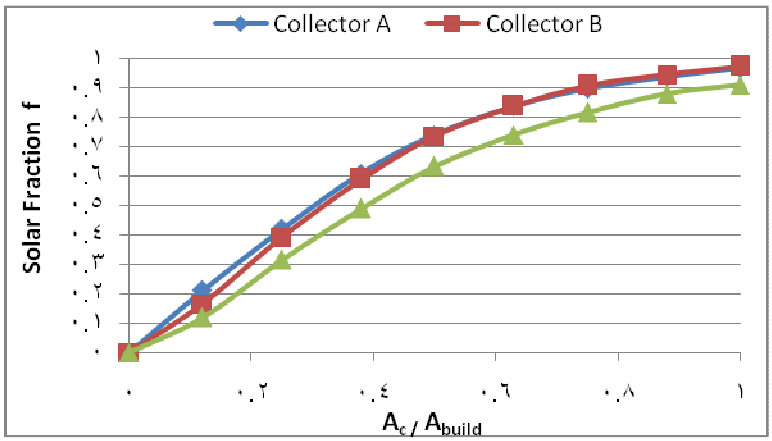

Figure 11: Relation between solar fraction and collector area for three type of collector

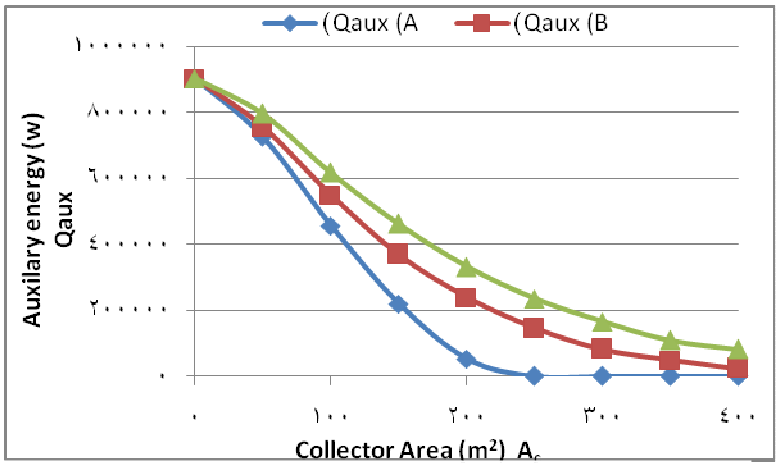

Figure 12: Relation between auxiliary energy and collector area for three type of collector

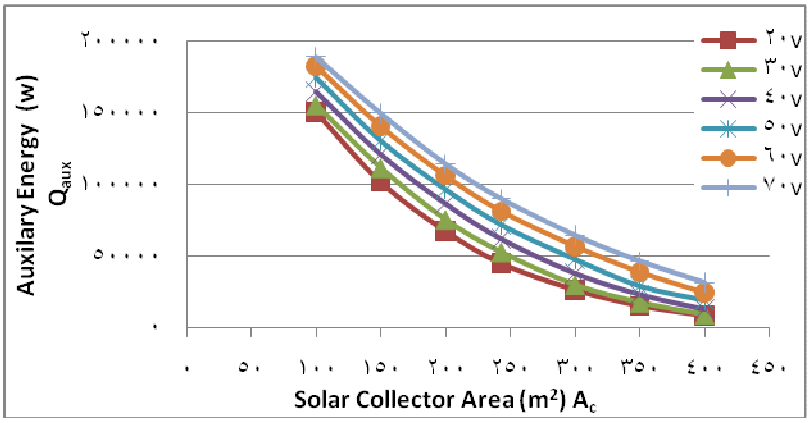

Figure 13: The relation between collector area versus auxiliary energy for different storage sizes

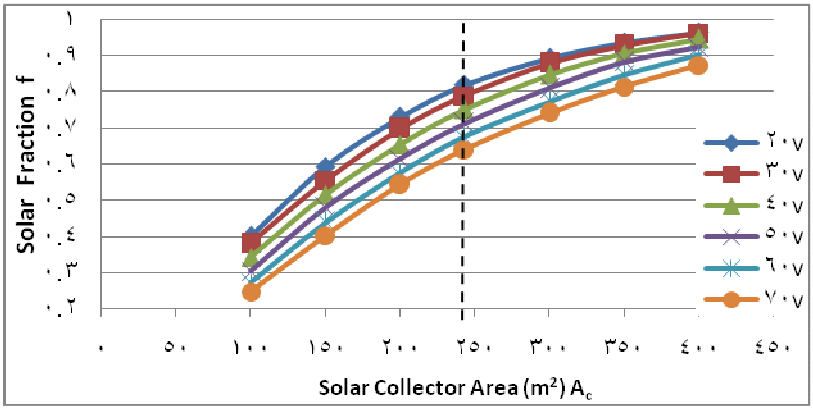

Figure 14: The Relation between collector are avers us solar fraction for different storage sizes

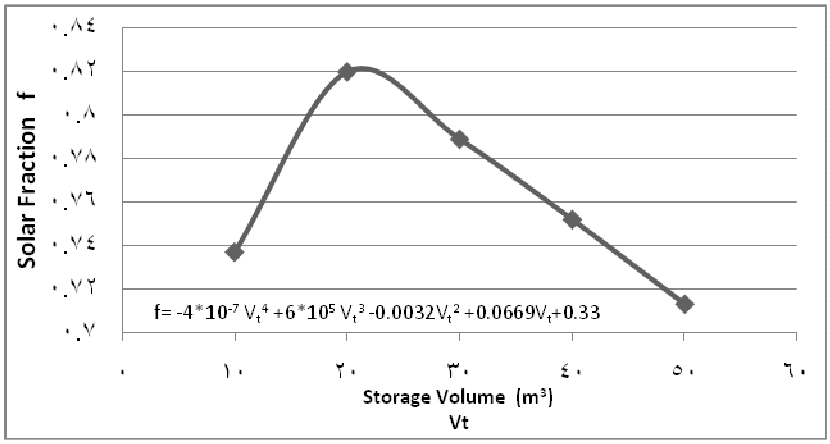

Figure 15: Relation between storage volume and solar fraction at collector area (243m^2)

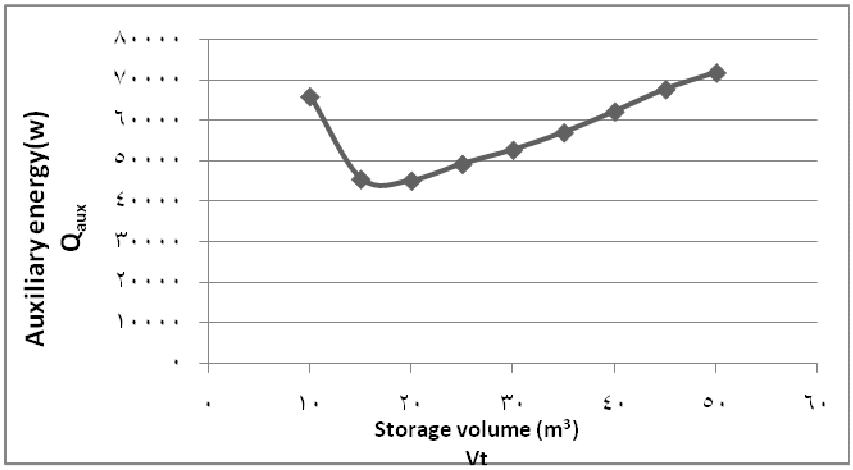

Figure 16: Relation between storage volume and auxiliary energy